On the Nonuniqueness of the Coupled Origin Time – Velocity Tomography Problem

By William Menke, R. Chadwick Holmes and Jiakang Xie

M S2005192 Version 2

Abstract. When earthquakes are used as sources in velocity tomography, the unknown velocity structure and the unknown hypocentral parameters (that is, source location and origin time) must be simultaneously estimated during the imaging process. This coupling allows the two sets of unknowns to trade off, and increases the degree of nonuniqueness of the resulting tomographic image above what would have been present had the hypocentral parameters been precisely known. We analyze, in detail, the nonuniqueness associate with unknown origin time, which we argue is often a more important source of nonuniqueness than is unknown location. While this type of nonuniqueness has long been understood to be a problem in teleseimic tomography, we show here that it is of equal importance in all coupled problems. We provide a practical method for calculating null solutions, and calculate them for several commonly-encountered experimental geometries. We also show that the attenuation tomography possesses a mathematically identical nonuniqueness, with unknown source amplitude being the analogue to unknown origin time.

Introduction. Since its development in the 1970's (Aki et al, 1976; Aki and Lee, 1976; Crosson, 1976), passive-source seismic tomography has become a standard technique for imaging earth structure. The method has been applied at both global (e.g. Pulliam et al., 1993) and regional scales (e.g. Thurber, 1983; Toomey and Foulger, 1989; Lees, 1992; Foxall et al., 1993; LeMeur et al, 1997; Ritsema et al., 1998; Toomey et al., 1998; Benoit et al., 2003). The key feature that distinguishes this type of tomography (hereafter called the *coupled problem*) from traditional active-source tomography is the use of earthquakes with initially unknown location and origin time, in contrast to precisely timed and located anthropogenic explosions. The source parameters (location and origin time of each source) are estimated, together with the earth's three dimensional seismic velocity structure during the inversion process.

Several well-known special cases of standard tomography (that is, tomography with known source parameters) have been very thoroughly studied, and form the basis for our intuition on the behavior of the much more complicated cases encountered in the actual practice. Radon's (1917) problem, in which seismic rays are limited to straight lines, is one such example. Its solution can be proven to be unique, provided that the ray coverage is complete (i.e. rays at all positions and orientations) (see, for example, Deans, 1983). Equally importantly, the non-uniqueness associated with missing rays can be assessed (e.g. Menke, 1985), and some notions formed about the likely effect of poor ray coverage, even in the case of curved rays.

The coupled problem potentially suffers from an additional nonuniquess associated with the trading off of velocity structure with source parameters. This problem was studied in its generality by Pavlis and Booker (1980) and Spencer and Gubbins (1980). Two important results of these studies are: 1) a method for separating the uniquely-determined part of the velocity structure (the resolvable part) from the part that can trade off with the source parameters (the unresolvable part); and 2) a procedure for partitioning the unknowns so as to yield an equation that involves only the velocity, not the source parameters (thus reducing the number of unknowns that need to be dealt with at any one time). However, the actual procedure, which requires fairly complicated manipulations of the matrices that appear in the mathematical formulation of the problem, is arguably not so helpful in informing one's intuition about the severity of the nonuniqueness that might be encountered in a typical application. Thus we focus here on a simpler version of the problem, namely the nonuniqueness associated with just one source parameter, origin time.

Aki et al. (1976) put forward a simple explanation of why nonuniqueness exists in the special case of teleseismic tomography. In this case, all sources are assumed to be very distant from the receivers, all the receivers are assumed to be nearby one another, the reference model is taken to be vertically-stratified, and only the velocity model near the receivers is allowed to vary (Figure 1). With these approximations, all rays from a common source are parallel to one another, at least in the variable part of the model. Any vertically-stratified velocity perturbation, δv, affects the traveltime of all members of a set of parallel rays equally. Thus, one can always find a set of origin time perturbations that have exactly the same effect on arrival time as a given vertically-stratified velocity perturbation. Origin time and velocity structure exactly trade off. Teleseismic tomography is thus completely insensitive to the vertically-stratified part of the earth's velocity structure, and can only make statements about *lateral* heterogeneity.

The teleseismic case is so elegant that one might be tempted to think that there is something special about it, and that the trading off of origin time and velocity structure occurs in that case, and no other. Such a notion is incorrect! As we show in detail below, every coupled problem suffers from this same nonuniqueness, regardless of source-receiver geometry. The only thing that is special about the teleseismic case is that the unresolvable part of the velocity structure – the vertically-stratified part - can be easily identified and described. Other source-receiver geometries have the same nonuniqueness, but more complicated patterns of unresolvable structure.

The plausibility of such an assertion can be increased by examining another special case of the coupled problem, one in which the sources are within the volume that is being imaged and where the velocity structure is allowed to vary at arbitrarily small spatial scales (Figure 2). Except in the rare case in which a ray from one source passes exactly through the location of another source, the source can always be surrounded by a small spherical velocity perturbation, δv, that will perturb the traveltimes of all rays from it equally and have no effect on the traveltime of any ray from any other source. Small heterogeneities co-located with the sources are unresolvable. This case represents a different extreme from teleseismic case, and yet it shares the same nonuniqueness. Only the pattern of the unresolvable part of the velocity structure is different. We now analyze the general case, demonstrating that it also shares this same nonuniqueness.

Formulation of the problem. Suppose that the arrival times of seismic rays from a set of events $\{i=1, \ldots P\}$ are observed at a set of receivers $\{j=1, \ldots Q\}$. After linearization about a reference earth model and reference origin time, the arrival time residuals, D_{ij}, are equal to the origin time residuals, x_i, plus a traveltime perturbation, Y_{ij}. To first order, the traveltime perturbation can be related to a set of velocity model perturbations, m_k, $\{k=1, \ldots R\}$ through a kernel, G_{ijk}. This kernel quantifies the effect on traveltime, Y_{ij}, of model parameter perturbation, m_k. Thus:

$$D_{ij} = x_i + Y_{ij} = x_i + \Sigma_k G_{ijk} m_k \qquad \text{(Eqn 1)}$$

Although correct, Eqn. 1 suffers from a notational problem, namely that the free indices of the terms do not match one another. We solve this problem by introducing the symbol w_j, defined as unity for all j. Then Eqn. 1 becomes:

$$D_{ij} = x_i\, w_j + \Sigma_k\, G_{ijk}\, m_k \qquad \text{(Eqn 2)}$$

In actual practice, the D_{ij}'s are measured quantities, the G_{ijk}'s are estimated from the reference model and the vectors **x** and **m** are unknown. The issue under consideration is the nonuniqueness of the solution of Eqn. 2, and especially the degree to which the values of **x** and **m** trade off. Just as in the two special cases considered above, we need to determine whether there is a model perturbation, **m**, that leads to the traveltime perturbation being equal for all rays having a common source. In other words, $\Sigma_k\, G_{ijk}\, m_k$ must vary only with indice, i, and not with indice, j. If such a solution can be found, then its effect on arrival time exactly mimics the effect of origin time, and the solution to Eqn. 2 must be nonunique.

Elimination of origin time residuals. Aki et al. (1976) introduced a procedure for eliminating **x** from Eqn. 1. First sum Eqn. 2 over j:

$$\Sigma_j\, D_{ij} = x_i\, \Sigma_j\, w_j + \Sigma_k\, \Sigma_j\, G_{ijk}\, m_k = x_i\, Q + \Sigma_k\, \Sigma_j\, G_{ijk}\, m_k \qquad \text{(Eqn 3)}$$

Here we have used the fact that $\Sigma_j\, w_j = Q$. We then divide by Q and rearrange:

$$x_i = (1/\,Q)\, \Sigma_j\, D_{ij} - (1/\,Q)\, \Sigma_k\, \Sigma_j\, G_{ijk}\, m_k \qquad \text{(Eqn 4)}$$

Eqn. 4 can now be used to eliminate x_i from Eqn. 2:

$$D_{ij} - (w_j/\,Q)\, \Sigma_p\, D_{ip} = \Sigma_k\, \{\, G_{ijk} - (w_j/Q)\, \Sigma_p\, G_{ipk}\, \}\, m_k \qquad \text{(Eqn 5)}$$

Note that we have rewritten several summations in terms of a dummy index, p, in order to avoid confusion. We have partitioned Eqn. 2 into two equations, Eqn. 5 for the model perturbations, **m**, (which can be solved first) and Eqn. 4 for the origin time residuals, **x**, (that can be computed once the model parameters have been determined). Note, however, that this manipulation does nothing to change the overall nonuniqueness of the problem. If Eqn. 5 has more than one solution, **m**, then there will be several pairs of (**x**, **m**) that solve Eqn. 1.

Construction of Null Solutions. We first rewrite the right hand side of Eqn. 5, using the previously-defined quantity, w_j, and the Kronecker delta, δ_{ij} (defined as unity if i=j and zero otherwise):

$$\begin{aligned}\Sigma_k \{ G_{ijk} - (w_j / Q)\, \Sigma_p G_{ipk} \}\, m_k &= \Sigma_k \{ \Sigma_p \delta_{pj} G_{ipk} - (w_j / Q)\, \Sigma_p G_{ipk} \}\, m_k \\ &= (1/Q)\, \Sigma_p \{Q\delta_{jp} - w_j w_p\} \{\Sigma_k G_{ipk} m_k\} = (1/Q)\Sigma_p A_{jp} B_{pi} \\ \text{with } A_{jp} = Q\delta_{jp} - w_j w_p &\text{ and } B_{pi} = \Sigma_k G_{ipk} m_k \end{aligned} \qquad \text{(Eqn 6)}$$

Note the use of the identity, $G_{ijk}=\Sigma_p\delta_{pj}G_{ipk}$. Note also that **A** is a symmetric Q×Q matrix with diagonal elements (Q−1) and off-diagonal elements (−1). Note also that **B** is a Q×P matrix and that it is a function of **m**. We now inquire whether there exist *null solutions*, $\mathbf{m}^{null}$, for which $\mathbf{AB}(\mathbf{m}^{null})=0$. If one or more of such solutions can be found, then Eqn. 5 is nonunique, since any linear combination of the null solutions can be added to a given solution without changing the value of the right hand side of the Eqn 5.

Evidently, two types of null solutions occur, those for which $\mathbf{B}(\mathbf{m}^{null})=0$ and those for which $\mathbf{B}\neq 0$ but $\mathbf{AB}(\mathbf{m}^{null})=0$. The former are just the null solutions to the underlying tomography problem, $D_{ij} = \Sigma_k G_{ijk} m_k$ (that is, Eqn. 1 without the origin time term). They represent unresolved velocity structure that has no effect on the traveltimes of any of the rays passing through the model. (They have no effect on the estimate of the origin time residuals, either). This kind of nonuniqueness, which we will call Type 1, is well-understood (see, for example, Menke 1989), and will not be discussed further here. The second kind of non-uniqueness, which we will call Type 2 and which we will examine in detail, below, is associated with the trading off of origin time and velocity structure.

We first consider the equation $\mathbf{A}\mathbf{v}=0$, where $\mathbf{v}$ is a non-zero vector. The solutions of this equation are the eigenvectors of $\mathbf{A}$ that correspond to zero eigenvalues (hereafter called the *zero eigenvectors*). One zero eigenvector is evidently $v_i=w_i$, since:

$$\Sigma_p A_{jp} v_p = \Sigma_p (Q\delta_{jp} - w_j w_p) w_p = Qw_j - Qw_j = 0 \tag{Eqn 7}$$

That this is the only zero eigenvector can be proven by establishing the equivalent fact that that $\mathbf{A}$ has a rank of Q–1. Remarkably, a closed form expression can be found for the upper-triangular form of $\mathbf{A}$ using standard Gaussian elimination. One starts with $\mathbf{A}$, which has diagonal elements (Q–1) and off-diagonal elements (–1). After creating the first column of zeros (not shown), the remaining (Q–1)×(Q–1) submatrix is found to have diagonal elements, (Q–2), and off-diagonal elements, (–1), both multiplied by an overall proportionality factor of Q/(Q–1). The triangularization process is recursive, and can continue until the 2×2 submatrix stage (but no further, since the last proportionality factor would be singular). The 2×2 submatrix is proportional to:

$$\begin{bmatrix} 1 & -1 \\ -1 & 1 \end{bmatrix} \quad \text{which triangularizes to} \quad \begin{bmatrix} 1 & -1 \\ 0 & 0 \end{bmatrix}$$

Precisely one row of the upper-triangle is zero, indicating that **A** has rank (Q−1).

Now consider the somewhat more complicated equation **AB**=0. We can view **A** as acting on the columns of **B**, individually (that is, on a series of vectors). Thus the equation will be satisfied if and only if each of these columns is proportional to the zero eigenvector. Thus $B_{pi} = w_p b_i$, where **b** is an arbitrary vector of length P of coefficients.

The null solutions, $\mathbf{m}^{null}$, therefore solve equation:

$$B_{pi} = \Sigma_k\, G_{ipk}\, m^{null}{}_k = w_p b_i \tag{Eqn. 8}$$

Eqn. 8 corresponds to solving the underlying tomography problem (that is, Eqn. 1 without the origin time term) for a specific choice of arrival time residuals, namely $D_{ij=} w_j b_i$. As discussed above, the solution defines a model perturbation corresponding to traveltime perturbations that are equal for all rays having a common source. In general, Eqn. 8 can be solved for any kernel, G_{ipk}, as long as R≥PQ, that is, there are at least as many model parameters as observations. The nonuniqueness is not limited to Aki et al.'s (1976) special case of teleseismic array geometry, but exists in all coupled origin time – tomography problems.

Given a specific tomography problem (that is, a particular pattern of sources and receivers), a reasonable strategy for studying the spatial pattern of the unresolvable part of the velocity structure is to solve Eqn. 8 P times in succession, with:

$$b_i=\delta_{iq},\ \{q=1, \ldots P\} \tag{Eqn. 9}$$

Then the q-th solution will quantify the effect of uncertainty in the origin time of the q-th event, with all other origin time perturbations held at zero. Any linear combination of these P solutions is also unresolvable.

In the special case where the underlying tomography problem is unique, then G_{ijk} has and inverse operator, $G^{-1}{}_{pqr}$, such that:

$$\Sigma_i \, \Sigma_p \, G^{-1}{}_{qip} \, G_{ipk} = \delta_{qk} \qquad \text{(Eqn 10)}$$

Then the null solutions are given explicitly by:

$$m^{null}{}_q = \Sigma_i \, \Sigma_p \, G^{-1}{}_{qip} b_i w_p \qquad \text{(Eqn 11)}$$

Implementation issues. Elimination of the origin time, as in Eqn. 5, does not eliminate the underlying trading off of origin time and velocity model perturbation. But in most actual implementations, the step at which one specific combination of origin time and velocity model perturbation is selected from among a myriad of possibilities is not clearly identified. This is because in solving Eqn. 5, the existence of Type 1 nonuniqueness still has to be contended with. The usual approach is to use damped-least squares, which selects the smallest **m** compatible with the equation (that is, the one that minimizes the L-2 norm of **m**). But actually, both Type 1 and Type 2 nonuniqueness are present, so the damping process implies a specific choice of **b** as well, namely **b**=0.

Aki et al. (1976) eliminated the origin time from Eqn. 1 in order to reduce the number of unknowns from R+P to R. This reduction was important at the time, given the small memory capacity of the computers of the 1970's. However, the process has a significant drawback: Eqn. 5 is much less sparse than Eqn. 2. Today, very efficient matrix solvers are available, such as those based on the biconjugate gradient method

(Press 1992), and their efficiency scales with the sparseness of the matrix. While they can be used to solve either Eqn. 1 or Eqn. 5 in the least squares sense, they will generally be much faster when applied to Eqn. 1 (Menke 2005). Thus a more modern approach is to solve Eqn. 1 for both origin time, **x**, and velocity perturbation, **m**, but to apply different damping factors to these two sets of unknowns, with their values chosen so that the solution with the smallest **m**, as contrasted to the smallest **x**, is selected. In this context, the actual values of the origin time perturbations are usually not themselves of interest; they are simply *slack variables* whose inclusion simplifies the solution of the tomography problem.

Examples of Null Solutions. We calculate the spatial pattern of null solutions, $\mathbf{m}^{null}{}_{p}$, for two commonly-encountered cases of source-receiver geometries, one with deep and the other with shallow sources. Both cases use a 17x17 array of receivers spaced 2.5 km apart along the topmost surface of the model and P=8 sources arranged to provide adequate azimuthal and angular coverage. The deep case, with a common source depth fixed at 49 km, is reminiscent of Aki et al. (1976) but with sub-parallel rays (Figure 3). One kilometer deep sources are used in the shallow case, with the sources mostly outside of the volume being imaged (the "undershooting" geometry used, for example, by Gudmundsson et al. 1994) (Figure 4). Synthetic traveltime data is calculated using Menke's (2005) RAYTRACE3D computer code. The reference model is defined in a 100×100×50 km region containing 51×51×51 nodes, and is linearly interpolated with tetrahedral defined by adjacent nodes. The reference velocity is taken to increase linearly with depth, from 3.0-8.0 km/s. Eqn. 8 is solved using a damped least-squares algorithm with R=18,225 model parameters, corresponding to nodal velocities within the upper-central part of the model (i.e. |x|, |y|, and z < 25 km). All P=8 null solutions, $\mathbf{m}^{null}{}_{p}$ {p=1, … 8}, are computed for each case study

A common feature of the eight solutions for the deep source case (Figure 3) is the distinct banded pattern in velocity anomalies with a wavelength of ~10 km. The scalloped character of the velocity anomalies is a direct result of balancing the delayed traveltimes of rays from the perturbed source while accommodating the traveltimes of subparallel rays from surrounding sources. The p=3 and p=4 solutions are reminiscent of a set of imbricate thrust faults, and highlight the potential danger in misinterpreting what is in fact a "model artifact" as a geological structure. The p=2 and p=8 solutions have a large central anomaly, that could be misconstrued as evidence for, say, mid-crustal melt.

The solution set for the shallow source case (Figure 4) illustrates the tendency for velocity anomalies to focus near the perturbed source location when the source is proximal to the edge of the imaged volume. Again we see indications of an oscillatory anomaly pattern (e.g. p=5 and p=8), which could be misinterpreted as crustal heterogeneities. Other solutions (e.g. 1, 4, and 6) are characterized by weaker isolated anomalies. This is because a broader spread in the source locations leads to a localization of the anomaly pattern. The turning depth for rays from each source controls the depth where velocity anomalies will be most pronounced in the null solution.

A typical real-world tomography problem would have more sources than the eight we employ here. As the number of sources is increased, the null solutions (not shown) become ever more oscillatory. This behavior results directly from Equation 9, the condition that the traveltime perturbation for rays emanating from one source be constant while perturbations from all the others sources – including nearby sources - be zero. However, this condition is only one acceptable choice among many. A choice that leads to less oscillatory solutions would be the requirement that traveltime perturbations from a group of nearby sources be similar, while those from more distant sources be zero. Then the null solutions of a problem with many sources would be similar to those with just a few sources. This behavior is related to the fact that any linear combination of null solutions is itself a null solution.

An alternative to explicit calculation of the null solutions is the calculation of several different tomographic inversions, each of which fit the data equally well, followed by an assessment of the differences between them. Such a set of solutions could be calculated, for instance, by using a suite of different damping and/or smoothing operators (e.g. Hammond and Toomey, 2003). Any differences between the inversions would be attributable to the presence of different amounts of null solutions in them. A limitation of this approach is that the set cannot be guaranteed to sample all the different null solutions, and may thus fail to identify all of the nonuniqueness inherent in the problem.

Application to Attenuation Tomography.

Attenuation tomography is a widely-used technique for imaging spatially-varying seismic attenuation, that is, the rate at which seismic energy is absorbed by frictional processes in different parts of the earth. It has been widely used to examine attenuation in many tectonic setting, including volcanic terrains (Zucca and Evans, 1992; Hansen et al. 2004), transform faulting (Lees and Lindley, 1994; Schlotterbeck and Abers, 2001), subduction (Roth et al., 1999; Stachnik et al. 2002), extensional plate boundaries (Wilcock et al.,1992; Menke et al., 1995) and continental interiors (Xie and Mitchell, 1990; Shi et al., 1996; Erickson et al. 2004).

In a homogeneous medium, the amplitude, $A(\omega)$, of a wave at angular frequency, ω, is often modeled as declining exponentially with traveltime, T, according to the formula:

$$A(\omega) = S(\omega)\, G\, R \exp\{-\tfrac{1}{2}\omega T Q^{-1}(\omega)\} \tag{Eqn 12}$$

Here $S(\omega)$ is the source spectral amplitude, G is the geometrical spreading factor, R quantifies the receiver site response, T is the travel time. $Q(\omega)$ is the quality factor, whose reciprocal, $q(\omega)= Q^{-1}(\omega)$ is proportional to the rate of energy absorption.

At frequencies at which ray theory is valid, Eqn. 12 can be extended to inhomogeneous media, where q varies with position, ξ, by replacing the quantity, $TQ^{-1}(\omega)$, with a path integral along the ray connecting event, i, and receiver, j. After taking a logarithm, Eqn. 12 becomes:

$$\ln(A_{ij}) = \ln(S_i(\omega)) + \ln(G_{ij} R_j) - \tfrac{1}{2}\omega \int_{ray_{ij}} q(\xi,\omega)\, dT \tag{Eqn 13}$$

To image the lateral variations of $q(\xi,\omega)$, the second term on the right-hand of Eqn. 13 ($\ln(G_{ij} R_j)$) is typically estimated and substracted from $\ln(A_{ij})$. Ideally the estimated $\ln(G_{ij} R_j)$ is accurate so Eqn. 13 becomes

$$\ln(A'_{ij}) = \ln(S_i(\omega)) - \tfrac{1}{2}\omega \int_{ray_{ij}} q(\xi,\omega)\, dT \tag{Eqn 14}$$

with the *reduced data* given by $\ln(A'ij)=\ln(A_{ij})-\ln(G_{ij}\ R_j)$.

Given a set of discrete model parameters, m_k, $\{k=1, \ldots R\}$that quantify the spatial variation of $q(\xi,\omega)$, the integral in Eqn. 13 can be approximated by a summation:

$$\ln(A'_{ij}) = \ln(S_i) - \tfrac{1}{2}\omega\ \Sigma_k\ G_{ijk}\ m_k \tag{Eqn 15}$$

Here the kernel, G_{ijk}, is a discrete version of the integrand of the ray integral. In the special case of discretization by voxels, then G_{ijk} would just represent the traveltime of ray (i,j) in voxel k.

We now note that Eqn. 15 has exactly the same form as Eqn. 2. Source strength plays the same role in the attenuation tomography as origin time plays in velocity tomography. Both problems share the same underlying non-uniqueness. Source strength and spatially-varying quality factor trade off in exactly the same way as origin time and spatially-varying velocity. The approach of Aki et al. (1976) for solving velocity problem has been extended to attenuation tomography to eliminate source amplitude term (Phillips and Hartse, 2002).

One special concern in attenuation tomography that noise in the reduced data, A'_{ij}, is often dominated by model error (that is, errors in the estimation of the geometrical spreading and site response terms in Equation 13), and not by measurement error (that is, error in measuring spectral amplitudes). Such errors are highly-correlated between observations and may not be normally-distributed. Highly-damped inversions are typically needed in such cases, and care must be taken that this damping does not obscure problems associated the underlying nonuniqueness of this tomography problem.

Discussion and Conclusions. The solutions to the coupled problem of simultaneously inverting seismic wave traveltimes for the source parameters (location and origin time) of earthquakes and the earth's seismic velocity structure are well-understood to be inherently nonunique (Pavlis and Booker, 1980; Spencer and Gubbins, 1980). Our investigation here has focused specifically on the nonuniqueness associated with origin time (as contrasted to location).

This type of nonuniqueness has long been supposed to be the most important type of uniqueness in Aki et al. (1976) style teleseismic tomography, because plausible mislocations of teleseismic earthquakes of a few tens of kilometers have little effect on the orientation of wavefronts impinging upon a distant receiver array. Indeed, very few practitioners of teleseismic tomography allow source locations (or, equivalently, plane wave incidence directions) to vary. Our work emphasizes the importance of origin time nonuniqueness in other forms of the coupled problem, as well. However, the relative importance of nonuniqueness associated with origin time and source location has not been thoroughly investigated in these cases.

Nevertheless, the following consideration suggests to us that origin time nonuniqueness will always be very important: In most practical applications, events at the periphery of the study area are an extremely important part of the overall dataset, because rays from such events sample the volume that is being imaged much more uniformly than rays from events located directly beneath the array. Rays from these events tend to lie in a fairly narrow cone of take-off angles, centered about an axis, ζ_1 (Figure 5). This is a well-studied special case in earthquake location theory. Even when the velocity model is held constant, the position of the event along the ζ_1 axis trades off very strongly with origin time. In this case, nonuniqueness associated with origin time and the ζ_1 component of location are equivalent – they have equal importance. On the other hand, we would not expect the position of the event in directions perpendicular to ζ_1 to trade off strongly with velocity structure, since perturbing the source location in this direction has negligible effect on the traveltimes of the rays.

The technique for exploring the unresolvable part of the earth's velocity structure that we develop here is easy to implement, because it only requires solving the underlying tomography problem for special sets of synthetic traveltimes. Plots of the resulting null solutions, $\mathbf{m}^{null}$, serve to build confidence in interpretations of the final tomographic image by indicating when specific spatial patterns of velocity anomalies could be artifacts of a poorly resolved inversion, as contrasted to representing true geological structure. We recommend that null solutions be routinely computed and examined as an integral part of the inversion process.

Acknowledgements. This research was supported by the National Science Foundation under award OCE02-21035. Lamont-Doherty Contribution Number 00000.

References

Aki, K., Y. Christoffersson and E. Husebye, Three-dimensional seismic structure under the Montana LASA, *Bull. Seism. Soc. Am. 66,* 501-524, 1976.

Aki, K. and W.H.K. Lee, Determination of three-dimensional velocity anomalies under a seismic array using first P arrival times from local earthquakes; 1, A homogeneous initial model, *J. Geophys. Res. 81,* 4381-4399. 1976.

Benoit, M.H., A.A. Nyblade, J.C. Vandecar and H. Gurrola, Upper mantle P wave velocity structure and transition zone thickness beneath the Arabian Shield, Geophys. Res. Lett., 30(10), 1531, doi:10.1029/2002GL016436, 2003.

Crosson, R.S. Crustal structure modeling of earthquake data; 1, Simultaneous least squares estimation of hypocenter and velocity parameters, *J. Geophys. Res. 81*, 3036-3046. 1976.

Deans, S. R. The Radon Transform and Some of Its Applications. New York: Wiley, 1983.

Erickson, D., D.E. McNamara and H.M. Benz, Frequency-dependent Lg Q within the continental United States, *Bull. Seism. Soc. Am. 94*, 1630-1643. 2004.

Foxall, W., A. Michelini, and T. V. McEvilly, Earthquake travel time tomography of the southern Santa Cruz Mountains: Control of fault rupture by lithological heterogeneity of the San Andreas fault zone, *J. Geophys. Res. 98,* 17,691–17,710, 1993.

Gudmundsson, O., B. Brandsdottir, W. Menke and H. Olafsson, The magma chamber of Katla volcano in the propagating volcanic zone of south Iceland revealed by seismic undershooting, *Geophys. J. Int. 119*, 227-296, 1994.

Hammond, W.C. and R. Toomey, Seismic velocity anisotropy and heterogeneity beneath the Mantle Electromagnetic and Tomography Eperiment (MELT) region of the East Pacific Rise from analysis of P and S body waves, J. Geophysical Research 108, 2003.

Hansen, S., C. Thurber, M. Mandernach, F. Haslinger and C. Doran, Seismic velocity and attenuation of the East Rift Zone and south flank of Kilauea Volcano, Hawaii, *Bull. Seism. Soc. Am. 94*, 1430-1440, 2004.

Lees, J.M. and G.T. Lindley, Three-dimensional attenuation tomography at Loma Prieta; inversion of t* for Q, *J. Geophys. Res. 99,* 6843-6863, 1994.

LeMeur, H., J. Virieux and P. Podvin, Seismic tomography of the Gulf of Corinth; a comparison of methods, in Tomography of the European region., B. Alessandrini (editor) Annali di Geofisica. 40; 1, Pages 1-24. 1997.

Menke, W., Imaging fault slip using teleseismic waveforms, analysis of a typical incomplete tomography experiment, *Geophys. J. R. Astr. Soc. 81*, 197-204, 1985.

Menke, W., *Geophysical Data Analysis, Revised Edition, Discrete Inverse Theory*, Academic Press, Orlando, 289 pp, 1989.

Menke, W., Case studies of seismic tomography and earthquake location in a regional context, submitted to Seismic Data Analysis and Imaging With Global and Local Arrays, Alan Levander and Guust Nolet, Eds., American Geophysical Union, in press, 2005.

Menke, W., V. Levin and R. Sethi, Seismic attenuation in the crust at the mid-Atlantic plate boundary in South-west Iceland, *Geophys. J. Int. 122,* 175-182, 1995.

Lees, J.M., The magma system of Mount St. Helens: non-linear high-resolution P-wave tomography, *J. Volcanol. Geotherm. Res. 53*, 103-116, 1992.

Pavlis, G.L, and J.R. Booker, The mixed discrete-continuous inverse problem; application to the simultaneous determination of earthquake hypocenters and velocity structure, *J. Geophys. Res. 85*, 4801-4810. 1980.

Phillips, W.S. and H.E. Hartse, Regional path calibration using multiple-station amplitude tomography, *Seism. Res. Lett. 73*, 228, 2002.

Pulliam, R. J., D. W. Vasco, and L. R. Johnson, Tomographic inversions for mantle P wave velocity structure based on the minimization of L2 and L1 norms of International Seismological Centre travel time residuals, *J. Geophys. Res. 98*, 699–734, 1993.

Press, W., *Numerical Recipes in C: The art of Scientific Computing, Second Edition,* Cambridge University Press, Cambridge, 994p, 1992.

Radon, J., Über die bestimmung von funktionen durch ihre integralwerte längs gewisser mannigfaltigkeiten, Berichte Sächsische Akadamie der Wissenschaften, Leipzig, Math.-Phys. Kl. 69, 262-267, 1917.

Ritsema, J., A.A. Nyblade, T.J. Owens, C.A. Langston and J.C. VanDecar (1998), Upper mantle seismic velocity structure beneath Tanzania, east Africa: Implications for the stability of cratonic lithosphere, *J. Geophys. Res. 103*, 21,201-21,213, 1998.

Roth E.G., D.A. Wiens, L. Dorman, J. Hildebrand, S. Webb, Seismic attenuation tomography of the Tonga-Fiji region using phase pair methods, *J. Geophys. Res. 104*, 4795-4809, 1999.

Schlotterbeck, B.A. and G.A. Abers, Three-dimensional attenuation variations in Southern California, *J. Geophys. Res. 106*, 30,719-30,735, 2001.

Shi, J., W.-Y. Kim and P.G. Richards, Variability of crustal attenuation in the Northeastern United States from Lg waves, *J. Geophys. Res. 101*, 25,231-25,242, 1996.

Spencer C. and D. Gubbins, Travel time inversion for simultaneous earthquake location and velocity structure determination in laterally varying media, *Geophys. J. Roy. Astr. Soc. 63,* 95-116, 1980.

Stachnik, J.C., G.A. Abers and D.H. Christensen, Seismic attenuation and source scaling from intermediate-depth earthquakes; BEAAR results from central Alaska, *Seism. Res. Lett. 73,* 233. 2002.

Thurber, C.E., Earthquake locations and three-dimensional crustal structure in the Coyote Lake area, Central California, *J. Geophys. Res. 88*, 8226-8236, 1983.

Toomey D.R. and G.R. Foulger, Tomographic inversion of local earthquake data from the Hengill-Grensdalur central volcano complex, Iceland, *J. Geophys. Res. 94*, 17,497-17,510. 1989.

Toomey, D.R., W.S.D. Wilcock, S.C. Solomon, W.C. Hammond and J.A. Orcutt, Mantle seismic structure beneath the MELT region of the East Pacific Rise from P and S wave tomography, *Science 280*, 1224-1227, 1998.

Wilcock, W.S.D., S.C.Solomon, G.M. Purdy and D.R. Toomey, The seismic attenuation structure of a fast-spreading mid-ocean ridge, *Science 258,* 1470-1474, 1992.

Xie, J. and B.J. Mitchell, A back-projection method for imaging large-scale lateral variations of Lg coda Q with application to continental Africa, *Geophys. J. Int. 100*, 161-181. 1990.

Zucca, J.J. and J.R. Evans, Active high-resolution compressional wave attenuation tomography at Newberry Volcano, central Cascade Range, *J. Geophys. Res. 97*, 11,047-11,055, 1992.

Figure Captions.

Fig. 1. (Left) Geometry of the Aki et al. (1976) teleseismic tomography case. (Right) Corresponding reference velocity is vertically-stratified. Note that the velocity perturbation, δv, affects the traveltime of all rays equally.

Fig. 2. Case of tomography where the sources are within the volume that is being imaged, and where velocity perturbations with arbitrarily small spatial scale are permitted. The spherically-symmetric perturbation, δv, centered on a source affects the traveltime of all rays from that source equally.

Fig. 3. (Left) Null solutions, $\mathbf{m}^{null}{}_{p}$ {p=1,...,8}, to the coupled problem for the deep source. The model is sliced vertically at y=0 and shows velocity perturbations with respect to the reference model. Scale bar units correspond to an origin time perturbation of 0.01 s. (Right) Source-receiver geometry projected onto the horizontal plane. A gray

box outlines the spatial extent of the 17×17 receiver array. Non-perturbed sources and the perturbed source are indicated by circle markers and a star, respectively.

Fig. 4. Null solutions, $\mathbf{m}^{null}{}_{p}$ {p=1,...,8}, to the inverse problem for the shallow source case. The model is sliced horizontally at z=2 km. Other symbols are the same as in Figure 3.

Fig.5. Case of source near the edge of the volume that is being imaged. Rays leave the source in a narrow cone of angles, so that it is possible to define an axis, ζ_1, that is approximately parallel to the rays. The axes, ζ_2 and ζ_3, are perpendicular to ζ_1. See text for further discussion.

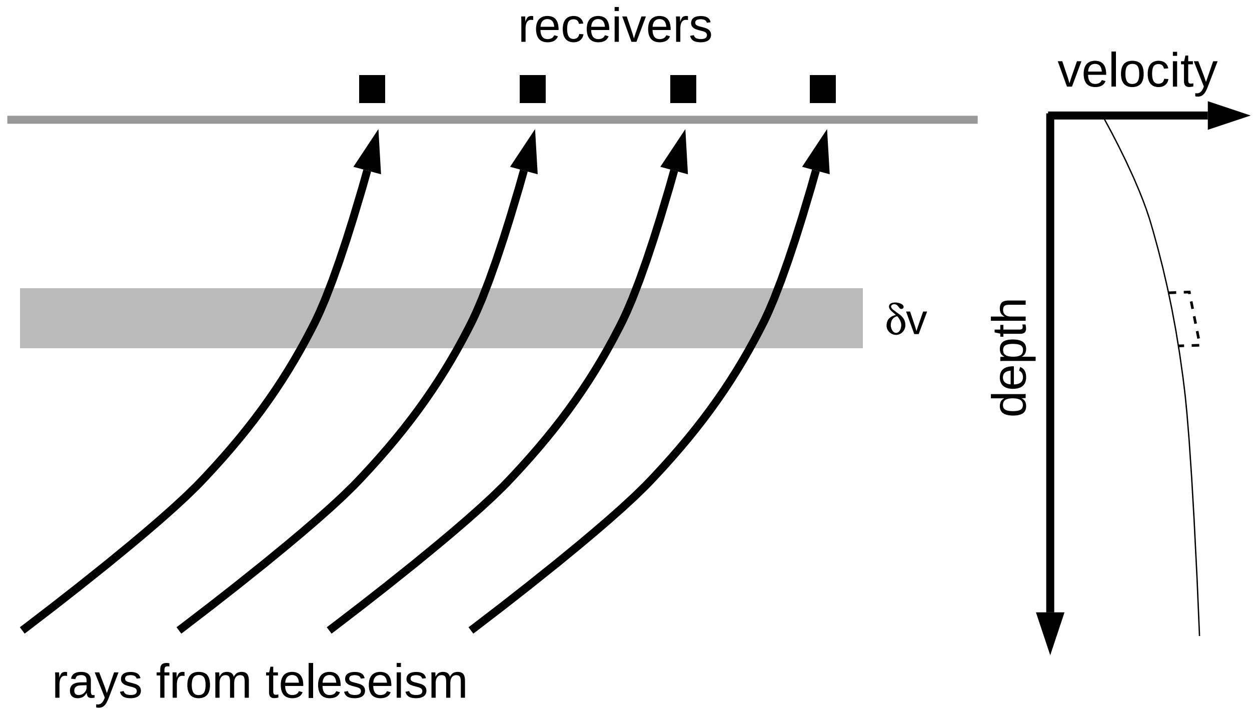
receivers
velocity
δv
depth
rays from teleseism

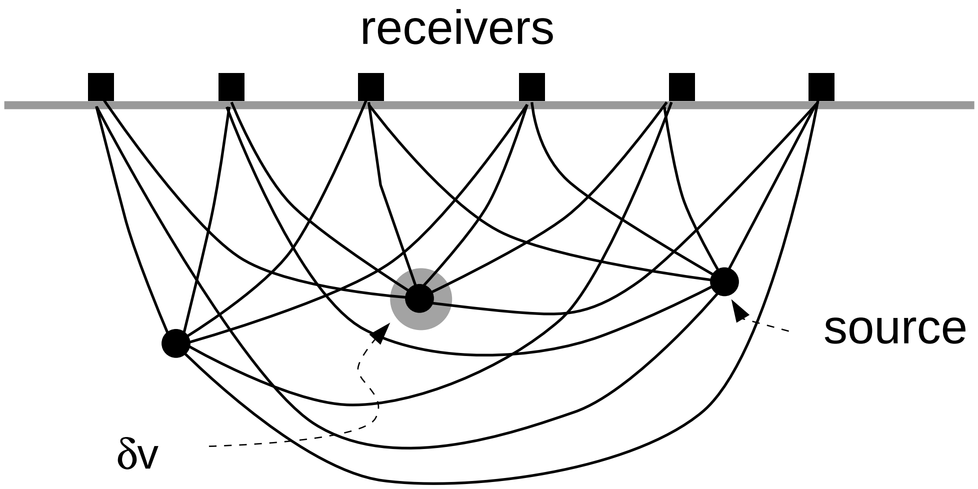
receivers
source
δv

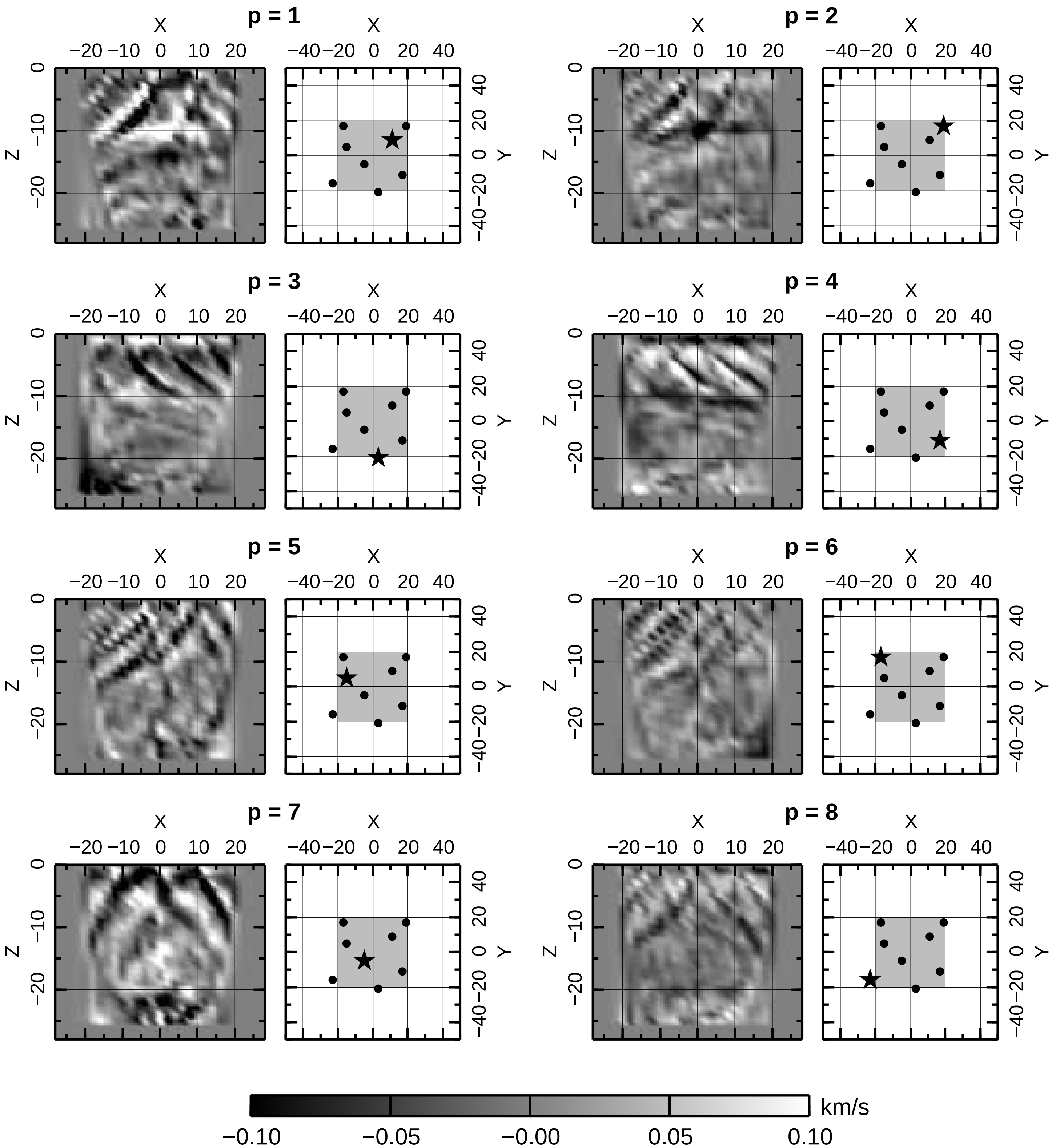
p = 1
p = 2
p = 3
p = 4
p = 5
p = 6
p = 7
p = 8
X
Z
Y
−20 −10 0 10 20
−40 −20 0 20 40
km/s
−0.10
−0.05
−0.00
0.05
0.10

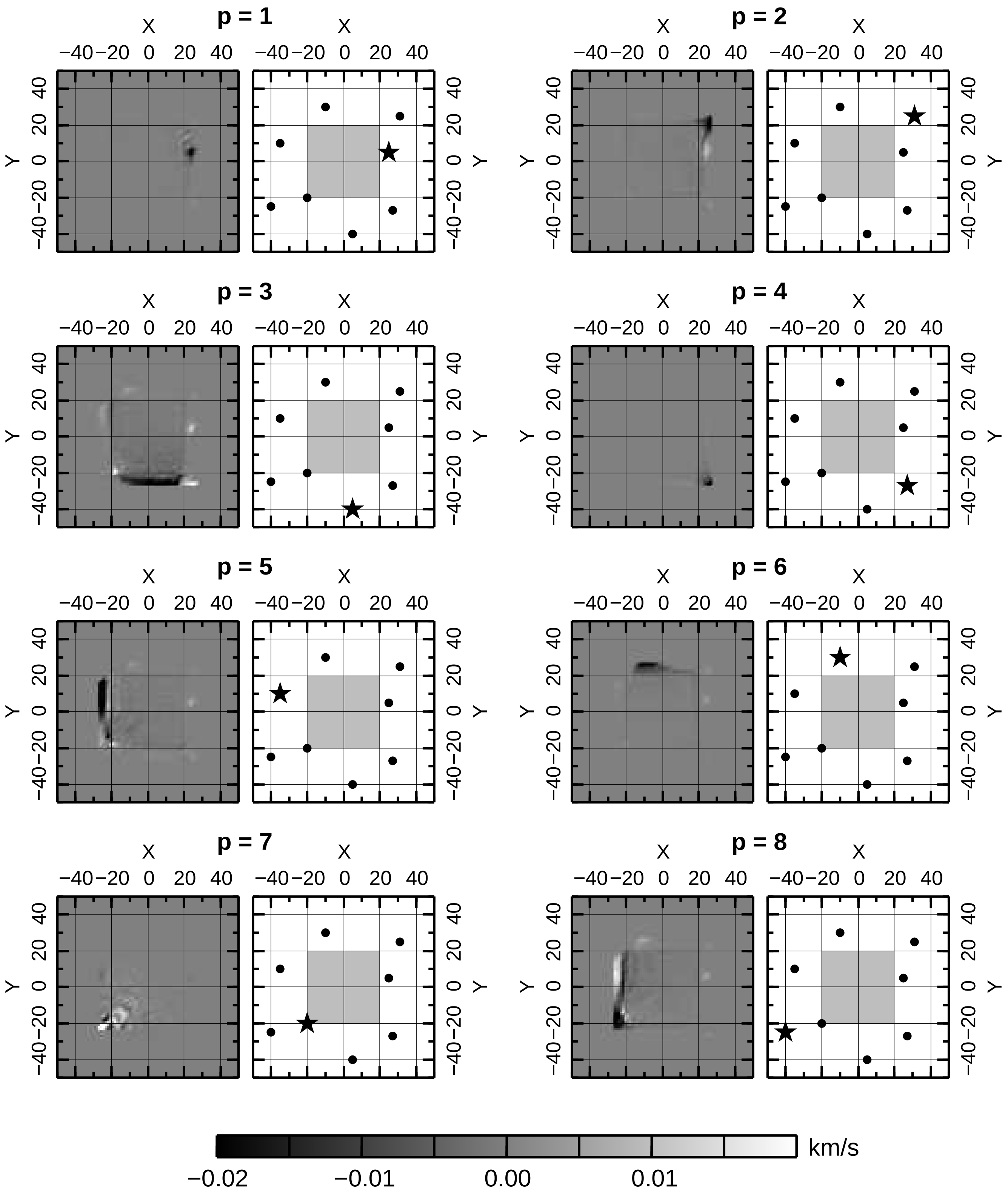

p = 1
p = 2
p = 3
p = 4
p = 5
p = 6
p = 7
p = 8
X
Y
−40 −20 0 20 40
km/s
−0.02
−0.01
0.00
0.01

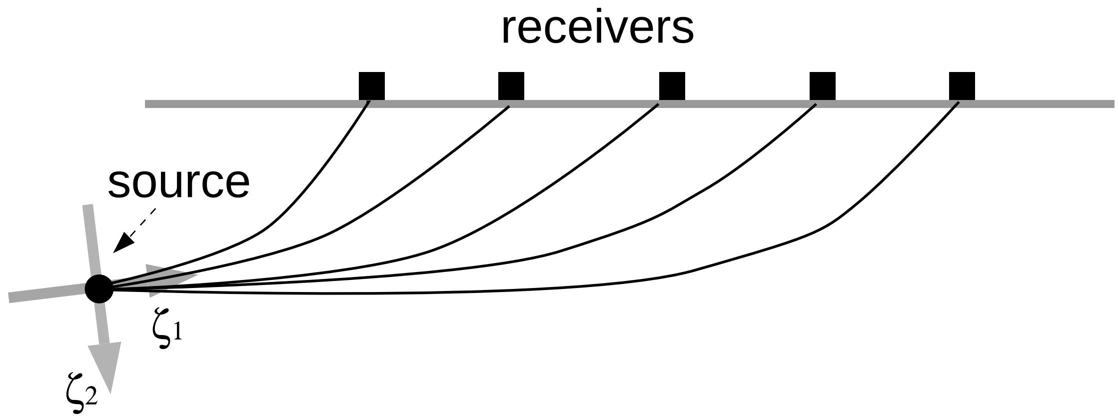
receivers
source
ζ_1
ζ_2